Theory of molecular tunneling ionization

X. M. Tong,* Z. X. Zhao, and C. D. Lin
Physics Department, Kansas State University, Manhattan, Kansas 66506
(Received 10 June 2002; published 20 September 2002)

We have extended the tunneling ionization model of Ammosov-Delone-Krainov (ADK) for atoms to diatomic molecules by considering the symmetry property and the asymptotic behavior of the molecular electronic wave function. The structure parameters of several molecules needed for calculating the ionization rates using this molecular ADK model have been obtained. The theory is applied to calculate the ratios of ionization signals for diatomic molecules with their companion atoms that have nearly identical binding energies. The origin of ionization suppression for some molecules has been identified. The predicted ratios for pairs with suppression (D_2:Ar, O_2:Xe) and pairs without suppression (N_2:Ar, CO:Kr) are in good agreement with the measurements. However, the theory predicts suppression for F_2:Ar, which is in disagreement with the experiment. The ionization signals of NO, S_2, and of SO have also been derived from the experimental data, and the results are also shown to be in agreement with the prediction of the present molecular ADK theory.

DOI: 10.1103/PhysRevA.66.033402 PACS number(s): 33.80.Rv, 42.50.Hz

I. INTRODUCTION

The ionization of an atom in an intense laser field has been investigated extensively in the last decades, both theoretically and experimentally. While direct solution of the Schrödinger equation in a time-dependent laser field has been widely used by theorists, simpler models are often preferable to experimentalists. One of the commonly used models for calculating the ionization rate is the so-called ADK (Ammosov-Delone-Krainov) model [1]. This model is based on the ionization rate of a hydrogenlike atom in a static electric field, with modifications introduced for the real many-electron atoms. A key element of the ADK theory is that the ionization rate depends critically on the ionization potential of the atom. Subsequent experimental studies of ionization of molecules have found that ionization rates for molecules, in general, are very similar to atoms if they have nearly identical binding energies. Further investigations have found exceptions [2–6]. These latter experiments showed that ionization is strongly suppressed for D_2 and O_2, in comparison with their companion atoms Ar and Xe, but ionization for N_2 and F_2 are comparable to their companion Ar atom under the same laser pulses. While *ab initio* calculations for the ionization rates of atoms are readily available, at least within the single-electron approximation, this is not the case for molecules. Based on the KFR (or Keldysh-Faisal-Reiss) model [7], the ionization rates for molecules have been calculated [8] in terms of ionization rates of atoms modified by the interference from the atomic centers. For ionization from an antibonding valence orbital, the interference is destructive and thus ionization is suppressed. For ionization from molecules in a bonding orbital, no suppression was expected. The ionization of molecules including many-electron effect has been studied based on the time-dependent density-functional theory by Chu and co-workers [9], but the complicated nature of these calculations sheds little light so far on the general issues of ionization suppression for molecules.

When considering the ionization of molecules versus atoms, effects due to the additional degrees of freedom in molecules should be evaluated. To begin with, the electronic cloud of an atom is spherically symmetric while for molecules it is not. The ionization rate of molecules can further be affected by the rotational and vibrational motion. While the exponential growth of ionization rates with field strength before reaching saturation is determined primarily by the ionization potential, the absolute ionization rates are determined by other properties of atoms and molecules. Thus in studying the ionization suppression of molecules, it is preferable to compare the ratio of ionization rates of molecules with respect to their companion atoms that have nearly identical binding energies. This is true also for experiments. As pointed out by DeWitt *et al.* [5] it is important to measure ionization signals of the companion atoms and molecules at the same time to reduce errors from variations of laser pulses in different shots.

Since the observation of ionization suppression of some molecules, different theoretical interpretations have been proposed. To explain the ionization suppression of D_2 in comparison to Ar (ionization energies of 15.4 eV and 15.8 eV, respectively), Talebpour *et al.* [3] attributed the suppression to the alignment of molecules. Such a claim is not supported by other studies [10]. For the simple H_2^+ molecular ions, quantum calculation [11] has shown that tunneling ionization rate does not depend strongly on the alignment of molecules. Saenz [10] has considered the possible effect on ionization suppression from the vibrational motion of molecules, but the effect was found to be too small. To explain the ionization suppression of O_2 in comparison to Xe (ionization energies at 12.06 and 12.13 eV, respectively), Guo [12] argued for a larger ''effective'' ionization potential for O_2, invoking that the open-shell nature of this molecule would result in the valence electron experiences a larger effective charge and a larger effective ionization potential (16.9 eV). The proposed larger ionization potential cannot be obtained theoretically, nor empirically from other experi-

*Email address: xmtong@phys.ksu.edu

ments. An alternative explanation of the suppression in O_2 was the interference model of Muth-Bohm *et al.* [8]. They used the Keldysh model for ionization where the initial molecular wave function is expressed as linear combination of atomic wave functions at the two centers. Using this approach they attributed the suppression in O_2 to the destructive interference of ionization from the two centers. They were able to use this model also to explain the different ejected electron spectra between Xe and O_2 [13]. This model, while being successful in explaining the suppression of O_2, fails to explain the suppression of D_2. The model would also predict suppression in F_2, but experimental result [5] shows no suppression in F_2.

As indicated earlier, a full *ab initio* theory for calculating the ionization of a molecule in a laser field is still not possible in the foreseeable future. In order to obtain a simple theory for calculating the ionization of molecules, we examined the basic models of the ADK theory for atoms and introduce modifications to develop a molecular ADK theory (MO-ADK), which can be used to calculate the ionization rate of molecules in a laser field. A simpler version of this model has been used earlier to explain the ionization suppression of O_2 and the lack of suppression for N_2. The theory has been used to calculate the saturation intensity of these molecules. In conjunction with the Lewenstein model [14], it was used to predict the high harmonic generation from molecules. With this theory, it is straightforward to predict that ionization suppression would result in an extension of the high harmonic cutoff, as observed experimentally in O_2 [15].

The purpose of the present paper is to provide a more complete description of the molecular ADK theory. It is based on the assumptions of the ADK model for tunneling ionization of atoms [1,16,17], but suitably modified to account for the difference in the electronic wave functions in atoms and molecules. Within this model, we investigate the effect of the alignment of molecules with respect to laser polarization. We also investigate the possible influence of the vibrational motion of molecules. The MO-ADK theory does not account for the many-electron effect, including the change of screening such as those discussed in the density-functional approach of Tong and Chu [18,19]. The theory also does not extend to regions where tunneling ionization is not the dominant ionization mechanism. In order to test the validity of the MO-ADK theory, we compare the calculated ionization signals for all the diatomic molecules that have been determined experimentally that we are aware of. The possible effects due to the temporal and spatial profiles of the laser pulses are also considered in order to make a valid comparison with experiments. Our predicted ratios of ionization signals for D_2:Ar, N_2:Ar, O_2:Xe, and CO:Kr are in good agreement with experiments. However, significant disagreement does occur for F_2:Ar. According to the present MO-ADK model, we would expect a suppression for F_2 in comparison with Ar. However, experiment [5] shows no suppression. For other molecules, such as, S_2, NO, and SO, there are no convenient atoms for comparison. We derived ''experimental'' ionization signals from existing data and showed that they are in agreement with the prediction of the present MO-ADK theory.

In Sec. II, the molecular ADK theory is derived and some parameters needed for calculating MO-ADK rates are tabulated. With these tabulated parameters for each molecule, the ionization rate for any laser pulses can be calculated with the same ease as the traditional ADK theory for atoms. The comparison with other calculations and the factors that affect the ionization signals are discussed in Sec. III. We then apply the MO-ADK theory to obtain ionization rates for diatomic molecules that have been measured. The results are presented and discussed in Sec. IV. The final section gives a summary and future outlook.

II. THE MOLECULAR ADK TUNNELING IONIZATION THEORY

The ADK theory for ionization of atoms in a laser field is based on the tunneling of an electron through the suppressed potential barrier of the combined atomic field and the external electric field. For a static electric field and for a hydrogenic atom the tunneling rate can be calculated analytically. The ADK theory is obtained by modifying the analytical formula by considering nonhydrogenic atoms. The chief among them is the modification of the radial wave function of the outermost electron in the asymptotic region where tunneling occurs. To obtain tunneling ionization rates for molecules, similar considerations on the electronic wave functions in the asymptotic region have to be considered. The ADK model for atoms was derived for an electronic state that initially has a well-defined spherical harmonics. To employ analytical expressions for the ionization rates for molecules, one has to express the molecular electronic wave functions in the asymptotic region in terms of summations of spherical harmonics in a one-center expansion.

In the molecular frame, the asymptotic wave function of a valence electron in a diatomic molecule at large distances can be expressed as (atomic units $m=\hbar=e=1$ are used thought the paper unless otherwise indicated)

$$\Psi^m(\mathbf{r})=\sum_l C_l F_l(r) Y_{lm}(\hat{\mathbf{r}}), \tag{1}$$

with m being the magnetic quantum number along the molecular axis. We normalize the coefficient C_l in such a way that the wave function in the asymptotic region can be expressed as

$$F_l(r\to\infty)\approx r^{Z_c/\kappa-1}e^{-\kappa r}, \tag{2}$$

with Z_c being the effective Coulomb charge, $\kappa=\sqrt{2I_p}$, and I_p being the ionization potential for the given valence orbital. Here, we assume that the molecular axis is aligned along the external field direction. The valence electron will be ionized along the field direction at $\theta\sim 0$. The leading term of the spherical harmonic along this direction is

$$Y_{lm}(\hat{\mathbf{r}})\simeq Q(l,m)\frac{1}{2^{|m|}|m|!}\sin^{|m|}\theta\frac{e^{im\phi}}{\sqrt{2\pi}}, \tag{3}$$

TABLE I. The ionization energy, equilibrium distance, and the C_l coefficients for diatomic molecules.

			C_l			
	I_p (eV)	R (Å)	$l=0$	$l=2$	$l=4$	
H_2^+ (σ_g)	29.99	1.058	4.37	0.05	0.00	
D_2 (σ_g)	15.47	0.742	2.51	0.06	0.00	
N_2 (σ_g)	15.58	1.098	2.02	0.78	0.04	
O_2 (π_g)	12.03	1.208		0.62	0.03	
F_2 (π_g)	15.70	1.412		1.17	0.13	
S_2 (π_g)	9.36	1.889		0.81	0.07	
	I_p (eV)	R (Å)	$l=0$	$l=1$	$l=2$	$l=3$
CO (σ)	14.01	1.128	1.43	0.76	0.28	0.02
NO (π)	9.26	1.151		0.22	0.41	0.01
SO (π)	10.29	1.481		0.41	−0.31	0.01

with

$$Q(l,m)=(-1)^m\sqrt{\frac{(2l+1)(l+|m|)!}{2(l-|m|)!}}. \tag{4}$$

The wave function in the tunneling region can be written as

$$\begin{aligned}\Psi^m(\mathbf{r}) &\simeq \sum_l C_l Y_{lm}(\hat{\mathbf{r}}) r^{Z_c/\kappa-1} e^{-\kappa r} \\ &\simeq \sum_l C_l Q(l,m) r^{Z_c/\kappa-1} e^{-\kappa r} \frac{\sin^{|m|}\theta}{2^{|m|}|m|!}\frac{e^{im\phi}}{\sqrt{2\pi}} \\ &\simeq B(m) r^{Z_c/\kappa-1} e^{-\kappa r}\ \frac{\sin^{|m|}\theta}{2^{|m|}|m|!} e\frac{e^{im\phi}}{\sqrt{2\pi}},\end{aligned} \tag{5}$$

with

$$B(m)=\sum_l C_l Q(l,m). \tag{6}$$

Following the same procedure used in Ref. [16], we obtain the tunneling ionization rate in a static field as

$$w_{stat}(F,0)=\frac{B^2(m)}{2^{|m|}|m|!}\frac{1}{\kappa^{2Z_c/\kappa-1}}\left(\frac{2\kappa^3}{F}\right)^{2Z_c/\kappa-|m|-1} e^{-2\kappa^3/3F}. \tag{7}$$

Note that in Eq. (7) we have corrected the error in the coefficients in Ref. [16]. If there is only one partial wave l, Eq. (7) returns to the atomic, case as shown in Ref. [17].

If the molecular axis is not aligned along the field direction, but at an arbitrary angle $\mathbf{R}$ with respect to the field direction, the $B(m)$ in Eq. (7) is expressed as

$$B(m')=\sum_l C_l D^l_{m',m}(\mathbf{R}) Q(l,m'), \tag{8}$$

with $D^l_{m',m}(\mathbf{R})$ being the rotation matrix and $\mathbf{R}$ the Euler angles between the molecular axis and the field direction. The static field ionization rate is

TABLE II. The C_l coefficients for rare-gas atoms. Note that the coefficients predicted by the ADK model are also presented.

	He ($1s$)	Ne ($2p$)	Ar ($3p$)	Kr ($4p$)	Xe ($5p$)
I_p (eV)	23.59	21.56	15.76	14.00	12.13
C_l	3.13	2.10	2.44	2.49	2.57
C_l(ADK)	2.67	2.52	2.19	2.04	1.86

$$w_{stat}(F,\mathbf{R})=\sum_{m'}\frac{B^2(m')}{2^{|m'|}|m'|!}\frac{1}{\kappa^{2Z_c/\kappa-1}} \times\left(\frac{2\kappa^3}{F}\right)^{2Z_c/\kappa-|m'|-1} e^{-2\kappa^3/3F}. \tag{9}$$

The ionization rate in a low frequency ac field is given by

$$w(F,\mathbf{R})=\left(\frac{3F}{\pi\kappa^3}\right)^{1/2} w_{stat}(F,\mathbf{R}). \tag{10}$$

where F is the peak field strength.

In the present work, we calculate the coefficients C_l for molecules by the multiple-scattering method [20–22]. In this method, the effective potential for the molecule is approximated as follows: (1) a central potential within each atomic sphere; (2) a central potential with the appropriate Coulombic tail outside a sphere that inscribes the atomic spheres; and (3) a constant potential in the interstitial region. The potential and the wave function can be obtained self-consistently for a fixed internuclear distance and electronic configuration. The calculated wave function for the valence electron is then fitted in the outside region to obtain the coefficients listed in Table I. One can obtain the parameters by fitting the valence electron wave function calculated by other methods as well.

For atoms, we did not use the coefficient C_l from the ADK [1] model. We use the actual value calculated based on the self-interaction free density-functional theory [23] for atoms. There are slight differences between the calculated coefficients and those from the ADK model, both are listed in Table II for comparison. Note that our definition of the ADK coefficients is somewhat different. With the coefficients C_l obtained, which are the property of the ground state, we can study molecular tunneling ionization for aligned as well as randomly distributed molecules. Note that the present theory can be easily extended to more complex polyatomic molecules.

Since we will focus on the comparison of single ionization of a diatomic molecule with its companion atom that has a similar ionization potential, we will investigate what factors affect the calculated ratio within the MO-ADK model. Suppose the molecule and atom have ionization potentials I_1 and I_2, respectively, the ratio of the ionization rate from Eq. (10) for the molecule vs the atom is

TABLE III. Ratios of single-ionization rates [Eqs. (12), (13), and (14)] for each diatomic molecule with its companion atom at the laser intensity of 10^{14} W/cm^2 for the upper group and of 2×10^{13} W/cm^2 for the lower group. See Eqs. (12), (13), and (14) for the definitions of A's and Eq. (11) for R.

	A_1	A_2	A_3	R
		$I=10^{14}$ W/cm^2		
D_2:Ar	0.31	0.88	0.42	0.14
O_2:Xe	0.38	0.03	0.74	0.01
N_2:Ar	0.84	1.04	1.31	1.15
F_2:Ar	3.96	0.02	1.09	0.09
CO:Kr	0.33	1.00	0.98	0.32
S_2:Xe	0.97	0.11	29.6	2.43
SO:Xe	0.11	0.07	9.92	0.08
NO:Xe	0.13	0.12	33.0	0.51
		$I=2\times10^{13}$ W/cm^2		
S_2:Xe	0.97	0.06	1946	90.5
SO:Xe	0.11	0.04	1690	7.44
NO:Xe	0.13	0.07	2485	22.6

$$R=\frac{W_{mol}(F)}{W_{atm}(F)}$$
$$=\frac{B_{mol}^2(m)}{2^{|m|}|m|!B_{atm}^2(0)}\frac{\kappa_2^{2Z_c/\kappa_2+1/2}}{\kappa_1^{2Z_c/\kappa_1+1/2}}\left(\frac{2\kappa_1^3}{F}\right)^{2Z_c/\kappa_1-|m|}$$
$$\times\left(\frac{F}{2\kappa_2^3}\right)^{2Z_c/\kappa_2}e^{-2(\kappa_1^3-\kappa_2^3)/3F}. \quad (11)$$

We have set $m=0$ for the ionization of atoms since higher values of m contribute little. For molecules, we considered the m (taken to be positive only) of the valence electron when the molecular axis is aligned with the laser field direction. For σ orbitals, $m=0$; for π orbital, $m=1$. From Eq. (11), we see that the ratio depends on

$$A_1=\frac{B_{mol}^2(m)}{2^{|m|}|m|!B_{atm}^2(0)}, \quad (12)$$

which depends only on the ground-state wave functions;

$$A_2=\frac{\kappa_2^{2Z_c/\kappa_2+1/2}}{\kappa_1^{2Z_c/\kappa_1+1/2}}\left(\frac{2\kappa_1^3}{F}\right)^{2Z_c/\kappa_1-|m|}\left(\frac{F}{2\kappa_2^3}\right)^{2Z_c/\kappa_2}, \quad (13)$$

which depends on the ionization potential and on the field strength in a power-law relation; and

$$A_3=e^{-2(\kappa_1^3-\kappa_2^3)/3F}, \quad (14)$$

which depends on the ionization potential and on the field strength in an exponential relation.

Table III shows A_1,A_2,A_3, and R for each pair at a laser intensity of 10^{14} W/cm^2. For molecules with lower ionization energies, the parameters were calculated at a lower intensity of 2×10^{13} W/cm^2. For heteronulcear diatomic molecules, the values in Table III are the average values for molecules aligned along the field in both directions. We will come back to these numbers when specific pairs are compared later.

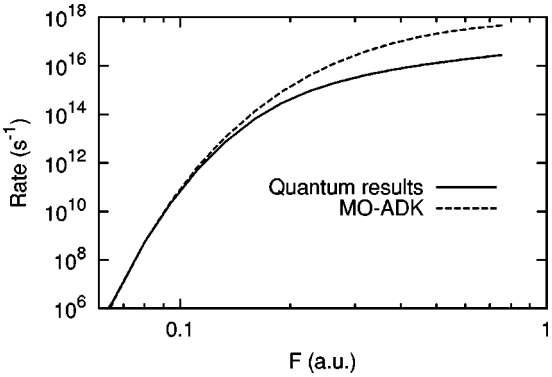

FIG. 1. Ionization rates of H_2^+ in a static field at the equilibrium distance. The solid curve is from the quantum result calculated using the complex rotation method [9].

III. THE VALIDITY OF THE MO-ADK THEORY AND OTHER FACTORS AFFECTING THE IONIZATION OF MOLECULES

A. Comparison of MO-ADK tunneling rate with other *ab inito* quantum calculations

The present MO-ADK ionization rate is an approximate tunneling ionization rate of a multielectron molecule at a fixed internuclear separation. While a full quantum theory of single ionization of a multielectron molecule has been formulated within the time-dependent density-functional theory by Chu and co-workers [24], such calculations are difficult to carry out and only few results have been reported. The key ingredient of the present MO-ADK model is the ionization rate of molecules in a static field [Eq. (7)]. Thus our first test of the MO-ADK theory is to compare with the quantum calculations for a one-electron H_2^+ ion in a static field.

We calculated the ionization rate of H_2^+ by the complex rotation method in prolate spheroidal coordinates in a similar procedure used by Chu and co-workers [9]. The MO-ADK rate is calculated by Eq. (7) with the H_2^+ parameters listed in Table I. Figure 1 shows the ionization rates calculated by two methods. In the lower-field region, the two results are in good agreement. The discrepancy starts from $F=0.2$ a.u. or $I>10^{15}$ W/cm^2. Beyond this field, the MO-ADK rate is larger than the value predicted by the quantum calculation indicating that in the overbarrier regime the tunneling model is no longer valid. On the other hand, this comparison shows that the present MO-ADK model works well in its region of validity.

In a recent paper, Saenz [25] calculated the ionization rate of neutral H_2 molecule in a static electric field where the molecular axis is aligned with the direction of the electric field. The calculation was performed including the correlation of the two electrons. We convert his calculated static rate to an ac rate using Eq. (10). In Fig. 2, we show that the MO-ADK rate for H_2 obtained from the present model is in

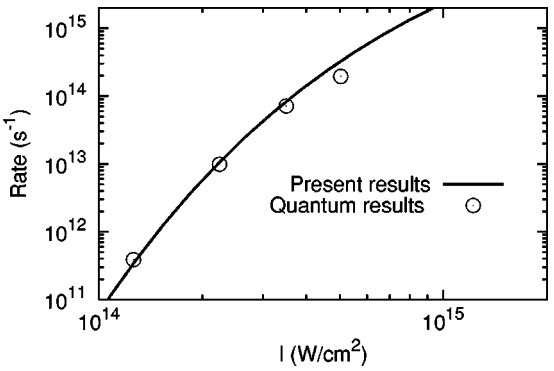

FIG. 2. Ionization rate of H_2 in an intense laser field at the equilibrium distance. The circles are from the *ab initio* calculations by Saenz [25].

good agreement with the full quantum calculations of Saenz [25]. The discrepancy appears in the higher laser intensity region only. So far we have compared the MO-ADK rate with the ionization rate of H_2^+ and H_2 in a static field. The comparison shows that the present MO-ADK model works in the tunneling region.

We note that Chu and co-workers [9] have studied the H_2^+ ionization in intense laser field by the Floquet method. Unfortunately, there are no data available for comparison from that work at the equilibrium distance.

B. Alignment effect on the ionization of molecules

It is well known that diatomic molecules can be aligned by linearly polarized lasers at low intensity (before ionization), if the pulse length is long enough (say over tens or hundreds of picoseconds). For short intense lasers it becomes more difficult to entangle the effect of alignment and the ionization of molecules separately. Within the MO-ADK theory the ionization rate for molecules oriented in different directions in space can be obtained from the ionization rate of molecules lined along the field direction through a rotation matrix, as explained in Sec. II. It is often assumed that ionization rate would be largest when the molecular axis is lined up with the field direction. This is actually not correct. The ionization rate is largest when the *initial electronic cloud* is aligned with the field direction. Not all diatomic molecules have their valence electronic orbitals lined along the molecular axis. For a π electron, for example, it is preferentially aligned in a direction perpendicular to the molecular axis.

To illustrate this effect, in Fig. 3 we show the ratios of single-ionization rates for N_2 and O_2 molecules aligned along the field direction over the rates when they are randomly oriented. Clearly we see that the ionization rate is enhanced for an aligned N_2 since its valence electron is a σ orbital, while for O_2 it is reduced since its valence electron is a π orbital. When we say molecules is aligned in a direction, we align the molecular axis. The tunneling ionization depends on the electron density. Thus for O_2 when the molecular axis is aligned in the field direction, the electronic cloud of the valence electron is not. Electrons that are mostly perpendicular to the field direction are difficult to ionize, thus the ionization is suppressed. It is a simple geometric effect.

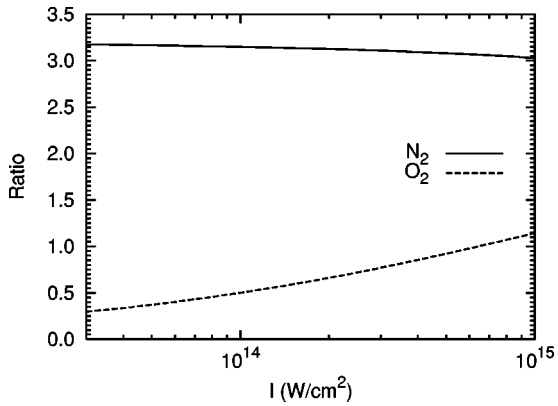

FIG. 3. Ratios of ionization rates for molecules aligned along the laser field direction over the randomly distributed ones. The solid line is for N_2 and the dashed line is for O_2.

C. Ionization rate, probability, and signal

In a pulsed laser field, the ionization rate depends on the peak field strength and laser's temporal and spatial profiles. It also depends on the molecular alignment, and most importantly the ionization energy. Since ionization is fast compared to the vibrational period, the ionization energy is taken to be the vertical ionization energy, which is a function of internuclear separation. To compare theoretical calculations with experimental ionization signals, all of these factors have to be included. For concreteness the electric field is taken to be that of a Gaussian beam. The electric field has the form

$$F(t,r,z)=\frac{F_0 W_0}{W(z)}e^{-2\ln 2\, r^2/W^2(z)}e^{-2\ln 2\, t^2/\tau^2},$$

with $W(z)=W_0\sqrt{1+z^2/z_R^2}$, where W_0 is the size of the focal spot, $z_R=\pi W_0^2/\lambda$ is the Rayleigh range, and λ is the laser wavelength. Here τ is the pulse length at full width at half maximum (FWHM) and F_0 is the laser field peak strength. If the molecule is aligned along direction $\mathbf{R}$, the ionization probability is expressed as

$$P(F,\mathbf{R})=1-e^{[-\int w(F,\mathbf{R})dt]}. \tag{15}$$

To compare with experiment, we need to calculate the ionization signal as

$$S_0(\mathbf{R})\propto\int P(F,\mathbf{R})2\pi r dr dz \tag{16}$$

for molecules that are aligned in a direction defined by the Euler angles $\mathbf{R}$. The integration in Eq. (16) can be performed on an equi-intensity surface [26]. This will reduce the two-dimensional integration to a one-dimensional integration. If the molecules are randomly distributed, the ionization signal is calculated as

$$S_1\propto\int S_0(\mathbf{R})d\mathbf{R}. \tag{17}$$

Figure 4 shows the ratio of single-ionization rates, probabilities, and signals from Eqs. (10), (15), and (17) for D_2:Ar for

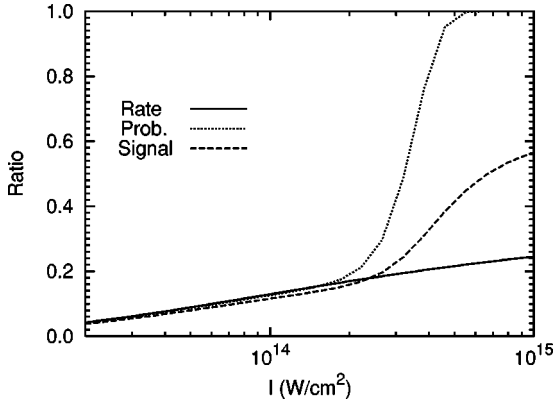

FIG. 4. Ratios of single-ionization rates, probabilities, and signals for D_2:Ar.

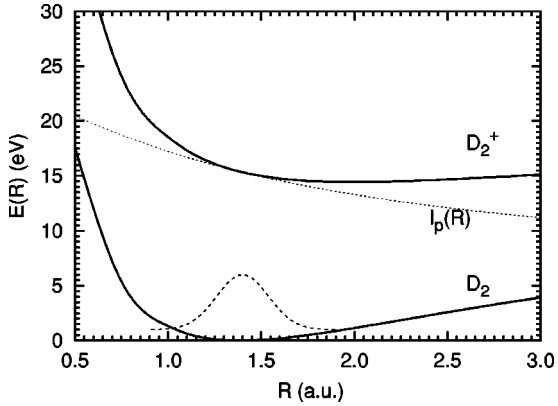

FIG. 5. Potential curves of D_2 and D_2^+ calculated from the Hartree-Fock method. The dotted line shows the vertical ionization energy as a function of the internuclear distance. The dashed curve shows the ground-state vibration density.

randomly distributed D_2 in a 25-fs pulsed laser. Clearly the ratios are close to each other before the field reaches the saturation intensity (at $I=3\times10^{14}$ W/cm^2). Around the saturation intensity, the ratio of probabilities increases dramatically and reaches the saturation value 1.0, while ratio of signals lies in between. Therefore, if the ionization probability is very small, the ionization signal is proportional to the integration of the ionization rate over the time and space as used in Ref. [27]. At the higher intensity, it is the ionization signal defined in Eq. (17) that corresponds to the experimental measurements.

D. Effect of vibrational motion

In experiments with short pulse lasers, i.e., for pulses of length of tens or hundreds of femtoseconds, the electronic transition occurs in a short time scale compared to the molecular vibration period, thus one should use the vertical ionization potential in the molecular tunneling model. If the vertical ionization potential changes significantly over the vibrational amplitude, then we need to fold the ionization signal over the vibrational distribution as

$$S_2 \propto \int S_1(R)\chi_v^2(R)dR, \tag{18}$$

where χ is the vibrational wave function. Figure 5 shows the potential curves for D_2^+ and D_2 calculated from the Hartree-Fock method [28]. The vertical ionization potential as a function of nuclear separation is shown. For the vibrational ground-state wave function, we use the harmonic-oscillator wave function where the vibrational frequency has been obtained from Raman spectra [29]. With the folding process, Eq. (18), we also investigated the effect of vibrational distribution on the MO-ADK rate.

IV. RESULTS AND DISCUSSION

Based on the present MO-ADK model, we have calculated the ionization ratios for homonuclear diatomic molecules with their companion atoms, D_2:Ar, N_2:Ar, O_2:Xe, and F_2:Ar; and heteronuclear diatomic molecules CO:Kr, NO:Xe, SO:Xe, and S_2:Xe. Each pair have nearly identical ionization potentials except for the last three. The ionization potentials and all the coefficients used in the MO-ADK calculations are listed in Tables I and II.

In our present calculation, we treat all the molecules to be randomly oriented. For the short pulses considered in this paper, simple estimate based on the static dipole polarizability of the molecules indicates that alignment would occur at a time scale longer than a few hundred femtoseconds. Nevertheless, the effect of alignment is to introduce a factor of 2 or 3 in the ionization rate. From the example in Fig. 3, the ionization rates for aligned molecules will increase if the tunneling is from the $m=0$ molecular orbitals, and decrease if it is from the $m=1$ molecular orbitals.

A. D_2:Ar

The ionization suppression of D_2 in comparison with Ar, which has a similar ionization potential, was first observed in the experiment by Talebpour *et al.* [3]. They interpreted the suppression as due to the random distribution of molecules with respect to the field direction. When the molecule is not lined up in the direction of the laser field, they derived an effective charge and a suppressed potential, and then used the ADK theory to calculate the ionization rate. The suppression derived using their model is too large. The suppression for this system has also been investigated by Saenz [10] by considering the effect of vibrational motion of the molecule. Although there was a suppression, the reduction was too small. In Fig. 6, we present the D_2:Ar single-ionization ratio vs the peak intensity of the laser, and compare the results with the measurement of Wells *et al.* [6]. Their data are consistent with the earlier measurements of Talebpour *et al.* [3]. It is clear that our calculations are in quite reasonable agreement with the data for intensity below 2×10^{14} W/cm^2. There are significant differences at the higher intensity which will be explained later. Note that the ionization potential we used here is the vertical transition energy, which is about 0.88 eV larger than the value listed in Table I.

In calculating the ionization ratio, we have included the spatial distribution of the laser intensity. The molecules are assumed to be randomly oriented. The possible effect due to

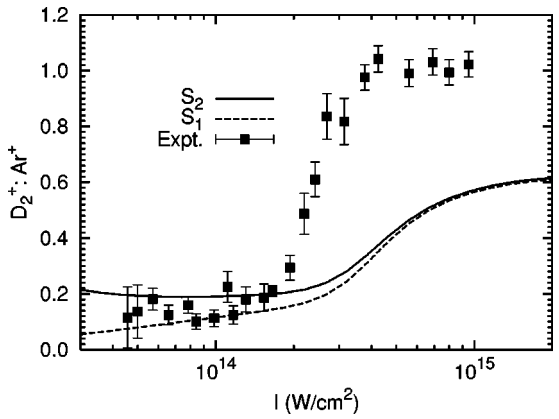

FIG. 6. Ratios of single-ionization signals of D_2:Ar vs the peak intensity of the laser field. The experimental data are from Wells *et al.* [6].

the vibrational motion is included (the S_2 curve), but the effect is not large. In other words, the present MO-ADK model is capable of explaining the suppression of D_2 ionization in comparison with Ar. However, what is the origin of ionization suppression in D_2?

According to the ADK theory, tunneling ionization rate is determined much by the suppressed barrier that occurs at a large distance from the atom. While the binding energy determines the tunneling probability each time the electron reaches the barrier, the frequency that an electron reaches the barrier is determined by the wave function in this asymptotic region. Equation (11) expresses the ratio of ionization rate in terms of the product of three terms. For D_2:Ar, A_3 would be 1.0 if the ionization energies were exactly identical. The small energy difference gives $A_3=0.42$ at the intensity of 10^{14} W/cm^2. The coefficient A_2, which is significant only when the m's in the tunneling model for the molecule are not zero, is essentially 1 for the present case. The ''suppression'' comes from the factors A_1 and A_3. The A_1 is 0.31, owing to the smaller electronic charge density for D_2 in the asymptotic region. This effect cannot be derived directly from the original ADK model for atoms without examining the electronic wave function of a molecule.

In Fig. 6, we notice that there is a large discrepancy between the present MO-ADK theory and the experimental data at higher intensity. From Wells *et al.* [6], it is known that D^+ formation becomes important for intensity above 2×10^{14} W/cm^2. The experimental signal contains this information but this contribution is not accounted for in the present theory.

B. O_2:Xe

The suppression of O_2 ionization with respect to Xe has been reported by Talebpour *et al.* [2] and by Guo *et al.* [30]. The O_2:Xe ionization ratio has been measured by DeWitt *et al.* [5] directly. While the ratio from DeWitt *et al.* is in general agreement with the ratio derived from the ionization signals reported by Guo *et al.*, we mention that the former can be up to a factor of 2 higher at lower fields. As discussed in the Introduction, the ionization suppression in O_2 has been explained by two earlier theoretical models. Mauth-Bohm *et al.* [8] attributed the suppression in O_2 to destructive interference from the two atomic centers since the valence orbital in O_2 is a π_g orbital. In another model, Guo [12] argued that the valence electron in O_2, because it is in an open shell, results in a larger effective charge and a larger effective binding energy, thus the ionization is suppressed. However, such an interpretation is not supported by calculations from the electronic structure of the O_2 molecule, nor from other experiments such as photoabsorption.

In an earlier paper [15], we showed that the ionization suppression of O_2 can be interpreted within the framework of the ADK model for atoms if one properly identifies the ''correct'' parameters in the ADK model when it is applied to molecules. It was noted that a two-center π_g orbital is closer to an atomic orbital with $m=1$ and $l=2$, when the atomic orbital is referred to the center of the molecule. According to this model, when O_2 is aligned in the direction of the laser field, the electron cloud is nearly perpendicular to the laser field and thus the ionization rate is very small. This simple observation explains the ionization suppression of O_2.

In the present MO-ADK model the valence electron wave function was calculated using the multiple-scattering theory. The asymptotic wave function, which is the essential ingredient for the ADK model, indeed has the dominant $m=1$ and $l=2$ character, as seen from Table I. The contributions from other l's are quite small. Among the three factors that contribute to the ionization ratio, the suppression comes from A_2, as seen from Table III. Note that the ionization potential we used here is the vertical transition energy that is about 0.33 eV larger than the value listed in Table I for O_2.

Based on the rates calculated from the present MO-ADK model, we compare the ratio of ionization signal of O_2 vs Xe. Clearly the results are in good agreement with the experiments within the spread of the data.

We mention that our interpretation of ionization suppression of O_2 is consistent with the interference model of Muth-Bohm *et al.* Both theories invoke the π_g character of the valence orbital. While Muth-Bohm *et al.* [8] emphasized the antibonding aspect and the destructive interference from the two atomic centers, our MO-ADK model attributes the suppression to the π character of the π_g orbital. Our model reflects the effect of electronic charge distribution with respect to the laser field direction, and has nothing to do with quantum interference. Further difference in actual calculations is that we used the ADK model for tunneling ionization and Muth-Bohm *et al.* used the KFR approximation for calculating the ionization rate.

We also emphasize that the origin of suppression in O_2 is different from that in D_2. Comparing O_2 with Xe within the MO-ADK model, $m=1$ for O_2 but $m=0$ for Xe such that the ratio of the ionization rate has an additional factor $(F/2\kappa^3)$ [see Eq. (7)], which grows with the laser field strength. This explains the relatively rapid rise of the ratio shown in Fig. 7 with intensity. For D_2, as explained earlier, the ionization suppression is due to the decrease of the *s*-wave radial function in the asymptotic region, not because of the angular dependence of the wave function in the asymptotic region as in O_2. Since $m=0$ for both D_2 and Ar

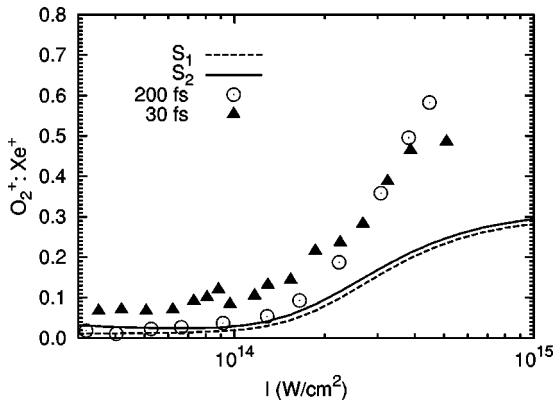

FIG. 7. Ratios of single-ionization signals of O_2:Xe vs the peak intensity of the laser field. The open circles are from the 200-fs pulse of Ref. [2] and the filled triangles are from the 30-fs pulse of Ref. [30].

in the MO-ADK theory, the ratio would be independent of laser intensity if the binding energy of D_2 and Ar were exactly identical.

C. N_2:Ar

We next discuss N_2 that is known to have similar ionization rate as Ar. The valence electron of N_2 also occupies a σ_g orbital like D_2. However, the σ_g orbital of N_2 is constructed from two $2p$ orbitals at the two centers, while for D_2 it is constructed from two $1s$ orbitals. Our calculation shows that the σ_g orbital in N_2 at large distance is a strong mixture of s wave and d wave, when expanded in terms of atomic orbitals at the center of the internuclear axis, see Table I. From Table III, we note that all the three $A_i(i=1-3)$ factors are near 1.0, showing no suppression from each factor. In other words, if the N_2 molecule is aligned along the field direction, its ionization rate would be identical to Ar. In fact, at the intensity of 10^{14} W/cm^2, the ratio was calculated to be 0.98, see Table III.

In Fig. 8, we show the ratio of ionization signal for N_2:Ar obtained from the present MO-ADK theory, assuming a randomly oriented ensemble of N_2 molecules and a Gaussian laser pulse of duration 25 fs. The results are compared to the ratio measured directly by DeWitt *et al.* [5], and to the ratios derived from the ionization signals measured by Guo *et al.* [30]. Clearly the two sets of experimental data differ by a factor of 3–4. Our calculated results are closer to the data of Guo *et al.* [30]. We emphasize that the calculations were presented for randomly distributed N_2 molecules. From Fig. 3, the ionization rate for a randomly distributed N_2 is about a factor of 3 smaller compared to the ionization rate for molecules aligned along the laser field direction.

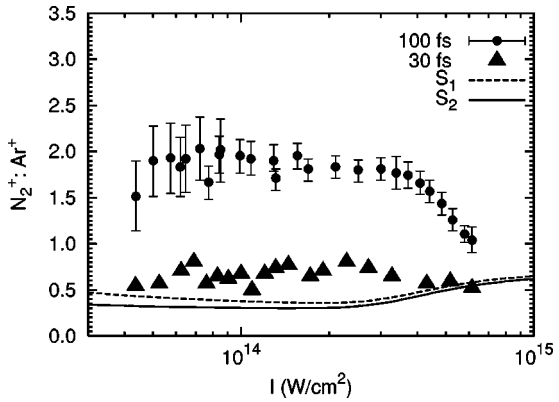

FIG. 8. Ratios of single-ionization signals of N_2:Ar vs the peak intensity of the laser field. The filled circles are from the 100-fs pulse of Ref. [5] and the filled triangles are from the 30-fs pulse of Ref. [30].

Is the difference of a factor of 3–4 in the ratio reported by DeWitt *et al.* and by Guo *et al.* bears any significance? (For O_2:Xe the difference is less than a factor of 2.) These two experiments used different pulse lengths, the former used a 100-fs pulse and the latter 30 fs. Could the difference in the ratio be due to the pulse length? From Eq. (15), when the ionization rate is small, the ratio of ionization probability will not depend on the pulse length. Thus we could not attribute the difference in the two experiments to the pulse length. On the other hand, calculations of Muth-Bohm [8] showed that the ratios for 30-fs pulse and 200-fs pulse are different.

For molecules, there is another possibility that ionization probability can depend on the pulse length. For a longer pulse, the molecule can be aligned before it is ionized. Using a simple model based on the static dipole polarizability for N_2, we did a classical calculation to estimate the possible alignment of N_2 in the field strength region studied by the experimentalists. We found that the molecules are neither aligned for the 30-fs pulse nor for the 100-fs pulse. Thus we tend to conclude that the difference in the ratios reported in the two experiments is a consequence of experimental uncertainties. In fact, the ratios reported from different experimental groups differ a great deal for this system, from 0.2 [31], 0.7 [30], 1 [13] to 1.7 [5].

Despite of the fact that our calculated ratios are closer to the data of Guo *et al.* [30], it is recognized that the ratio determined directly in DeWitt *et al.* [5] is supposed to eliminate errors introduced by differences in the laser intensities from shots to shots. The latter experimental data gave a ratio of 1.7 while our calculation gives a ratio of 0.4. The reduction of our ratio from 1.0 to 0.4 is due to average over the orientation of molecules. To reach the ratio of 1.7 reported in the experiment of DeWitt *et al.* [5], the ionization rate for an aligned N_2 has to be five or six times larger than Ar. Since the major error in the MO-ADK model comes from the calculation of the coefficients C_l's in Table I, which are estimated to have an error at the 20% level, the five to six times larger ionization rate for aligned N_2 molecules is not possible within the ADK tunneling model. We have also checked the possible effect from the vibrational motion of the N_2 molecule, but the effect was found to be small too. For the latter, we obtained the ionization potential from the total-energy difference of the neutral and molecular ions by the Hartree-Fock method [28].

D. F_2:Ar

The ionization of F_2 has been calculated using the interference model by Muth-Bohm *et al.* [8], where suppression

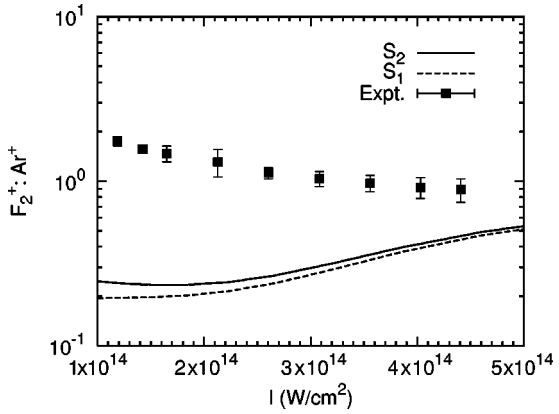

FIG. 9. Ratios of single-ionization signals of F_2:Ar vs the peak intensity of the laser field. The experimental data are from DeWitt *et al.* [5].

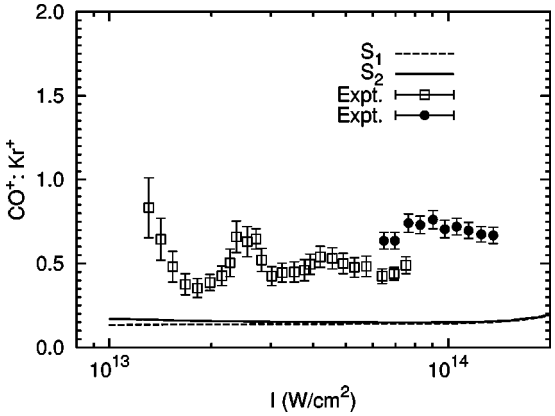

FIG. 10. Ratios of single-ionization signals of CO:Kr vs the peak intensity of the laser field. The experimental data are from Wells *et al.* [6].

with respect to Ar was predicted. Subsequent measurement by DeWitt *et al.* [5], however, showed that there is no ionization suppression for F_2. For field intensity in the range $(1-5)\times10^{14}$ W/cm^2, the F_2:Ar ratio drops by a factor of 2, from about 1.7–0.8, see Fig. 9.

What is the prediction of the MO-ADK model? The valence electrons are in the π_g orbital, like in O_2, except that there are four electrons in F_2 and only two in O_2. The fact that the former is a closed shell and the latter is an open-shell molecule does not matter within the present MO-ADK theory since it is a one-electron model. From Fig. 9, the MO-ADK model also predicts ionization suppression, in agreement with the interference model, but in total disagreement with the experimental data of DeWitt *et al.* [5]. From Fig. 9, we conclude that the MO-ADK theory predicts a ratio that is about a factor of 10 too low at 1×10^{14} W/cm^2 to a factor of 3 too low at 5×10^{14} W/cm^2. We have searched for possible effects that would increase the ionization rates from ionization of inner-shell electrons and from the effect of vibrational motion. These effects were found to be quite small. We will return to discuss other possible explanations for the discrepancy at the end of this section.

E. CO:Kr

The ionization of CO vs Kr has been measured by Wells *et al.* [6]. Their results are shown in Fig. 10, together with the prediction of the MO-ADK theory. The valence orbital of CO is a σ orbital and it is dominated by the *s* wave in the asymptotic region (see Table I). Therefore there is no suppression. The agreement between the calculations and the measurement is quite adequate. We mention that the agreement between theory and the experiment of Wells *et al.* [6] for the present case is comparable to the agreement between theory and the data of DeWitt *et al.* [5] for the N_2:Ar system.

F. NO:Xe, S_2:Xe, and SO:Xe

The ionization ratios of NO, SO, and S_2 vs Xe have been determined by Wells *et al.* [6]. Note that the ionization energy of Xe at 12.13 eV is somewhat higher than the 9.26 eV for NO, 10.29 eV for SO, and 9.36 eV for S_2. There are no convenient atoms with ionization energies in this range. Comparing systems with distinct ionization energies would mean that the ionization ratio be quite large at the same laser intensity, as in the present case. According to the MO-ADK model, we expect all three molecules to show ionization suppression since they all have π orbitals. From Table III, at the intensity of 2×10^{13} W/cm^2, the suppression from the π orbital reduces A_2 to a few percents, but the large difference in ionization energies result in large values of A_3, such that the ionization ratios at the same laser intensity are quite large.

How does the prediction from the MO-ADK theory compared to the measurements of Wells *et al.* [6]? It turns out that the ratios for these molecules measured are in the range of 1–10 smaller than what the MO-ADK theory has predicted, which are up to a factor of 100 or more at lower intensities near 10^{13} W/cm^2. We have traced that the errors in the ratios are not from the MO-ADK theory itself. Rather, it is from the failure of the ADK theory for Xe at the lower laser intensities covered in the experiment where multiphoton ionization begins to dominate. From the measurement of Guo *et al.* [4], the ADK theory has been shown to break down for intensity below 5×10^{13} W/cm^2. Due to the exponential dependence of the ionization rate on the intensity, the error of the ADK theory was found to be up to about 10^2 too low at 10^{13} W/cm^2. Since the critical intensity where the ADK model breaks down depends on the ionization energy, it becomes undesirable to present the ratios of ionization signals if one is interested in testing the validity of the present MO-ADK theory.

From the data of Wells *et al.* [6] and of Guo *et al.* [30], we derived an ''experimental'' ionization signal for each molecule at a given intensity for a 25-fs pulse used in the present calculation. Since these experiments were performed at different pulse lengths, we made the following two assumptions in deriving the ''experimental'' data: (1) the measured ionization ratios of NO:Xe, SO:Xe, and S_2:Xe are independent of the pulse length; (2) the ratio of the measured ionization signal of Xe as compared to the prediction from the ADK model for Xe is independent of the pulse length. From these two assumptions we ''derive'' the experimental

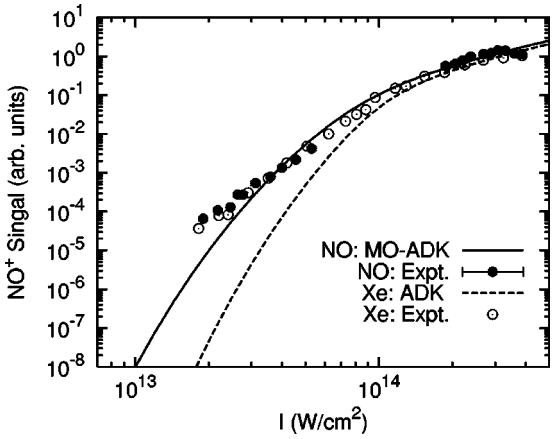

FIG. 11. The deduced ''experimental'' ionization signals for NO and Xe in a 25-fs Ti:sapphire laser pulse. The solid line is from the MO-ADK theory for NO and the dashed line is from the present ADK theory for Xe. See text for the derived of the experimental data.

ionization signal for a 25-fs pulse, which are then compared to the predictions of the MO-ADK theory. The results are shown in Figs. 11–13 for NO, S_2, and SO, respectively. In each figure we also show the ''experimental'' ionization signal for Xe at 25 fs and the prediction from the ADK model.

From Fig. 11, we note that the predicted ionization signals from the present MO-ADK theory are in good agreement with the deduced experimental data. In the measurement of Wells *et al.* [6] the data in the higher intensity region were taken with the 800-nm Ti:sapphire lasers, while the lower intensity region were taken after the wavelength had been doubled.

In Fig. 12, we note that the MO-ADK theory also predicts results that are in quite good agreement with the experimental data. Note that S_2 and NO have nearly identical binding energies. The difference, according to the present MO-ADK theory, is that the molecular orbital for the former is a *d* wave, while for the latter it is a mixture of *p* wave and *d* wave, see Table I. Due to the lower ionization energies for NO and S_2, the good agreement between the prediction of the MO-ADK theory and the deduced experimental results

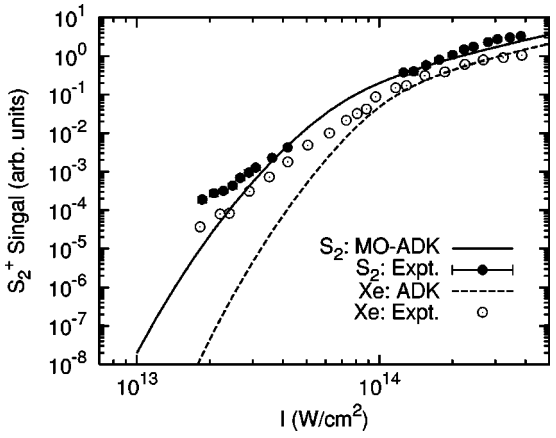

FIG. 12. Same as Fig. 11 but for S_2.

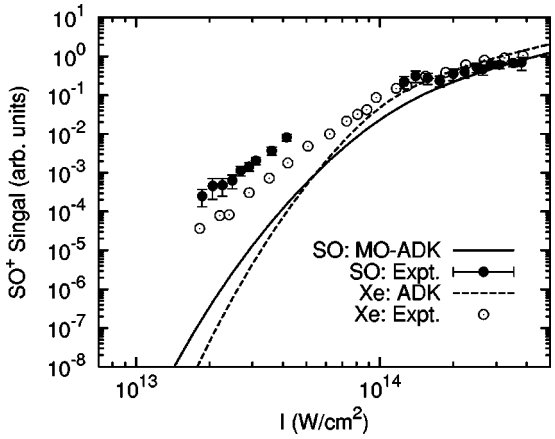

FIG. 13. Same as Fig. 11 but for SO.

indicates that the ionization of both molecules is still governed by the tunneling ionization mechanism for field intensities covered in the figures. However, in the lower intensity region, the ionization of Xe is no longer governed by tunneling ionization.

In Fig. 13, we note that the results from the present MO-ADK theory are lower than the deduced experimental ionization signals in the lower-field region. The ionization energy of SO is about 1 eV higher than NO and S_2. Thus for the same laser intensity, the dominant ionization mechanism for SO is no longer tunneling ionization. The discrepancy is ''acceptable'' since we expect that when the ADK model fails at the lower intensity it would predict a rate or signal that is too low as multiphoton ionization begins to contribute to the ionization mechanism.

G. On the discrepancy between theory and experiments

From the results presented in this section, it is clear that the MO-ADK theory has been able to explain the ionization ratios measured for quite a few number of molecules, including molecules that exhibit suppressions, i.e., D_2:Ar and O_2:Xe, and those not, i.e., N_2:Ar and CO:Ar. These pairs have nearly identical ionization energies and the comparison of the ionization ratios directly reveal the role of the electronic structure played in the tunneling ionization of molecules. The one lone exception is F_2:Ar where the MO-ADK theory predicts suppression, but the experimental result from DeWitt *et al.* [5] shows clearly that there is no suppression. The MO-ADK theory prediction is about a factor of 10 too small at lower intensity and a factor of 3 smaller at the higher intensity.

We have also calculated the ionization signals for NO, SO, and S_2 and compare them to the signals for Xe. We showed that the present MO-ADK theory also works well for these molecules. For SO, the discrepancy at the lower laser intensity can be attributed to the possible contribution from the multiphoton process.

Among the diatomic molecules examined here, it appears that only the F_2 data cannot be interpreted by the present MO-ADK theory. It will be of interest to see further theoretical and experimental work on this molecule. A more complete calculation based on the time-dependent density-

functional theory similar to what has been done for N_2 [24] would be useful. Similarly, further experiments at the same and different wavelengths on F_2 would also be of interest.

We comment that the failure of the ADK model for predicting the ionization rate of Xe for intensity below 5×10^{13} W/cm^2 should have little effect on the ratios for O_2:Xe presented in Fig. 7. These two have nearly identical ionization energies and we expect when the ADK model fails, it would occur more or less at the same laser intensity.

V. SUMMARY AND CONCLUSIONS

In this paper we developed a tunneling ionization theory for molecules based on the ADK theory, which has been widely successful for atoms. By examining the asymptotic wave function of the electron at a distance far away from the center of the molecule, the appropriate parameters that should be used for the ADK theory for molecules have been tabulated. With these parameters we show that ionization suppression of molecules can be anticipated when the valence electrons are in the π orbitals. The suppression originates from the fact that the electronic cloud for these molecules lies perpendicular to the molecular axis. Thus when the molecules are aligned along the laser field direction, the tunneling probability is small. Most of the molecules examined in this paper have suppression originating from the π character of its valence orbital. The only exception we have found so far is F_2 that has an outermost π orbital, but show no suppression. We have also identified suppression due to the reduction of electron density in the asymptotic region due to the binding of the electron in the ''molecular'' region. Such suppression is found in D_2. To conclude, the present MO-ADK theory provides an accurate and efficient theoretical model for calculating the ionization rates of diatomic molecules. The model can be extended to polyatomic molecules with ease and work is in progress, which can further test the validity of the present model.

ACKNOWLEDGMENTS

This work was supported in part by Chemical Sciences, Geosciences and Biosciences Division, Office of Basic Energy Sciences, Office of Science, and U. S. Department of Energy. CDL would like to thank Dr. Eric Wells and Dr. Bob Jones for communicating their data prior to publications and for the many discussions.

[1] M.V. Ammosov, N.B. Delone, and V.P. Krainov, Zh. Eksp. Teor. Fiz. **91**, 2008 (1986) [Sov. Phys. JETP **64**, 1191 (1986)].
[2] A. Talebpour, C.Y. Chien, and S.L. Chin, J. Phys. B **29**, L677 (1996).
[3] A. Talebpour, S. Larochelle, and S.L. Chin, J. Phys. B **31**, L49 (1998).
[4] D.S. Guo, R.R. Freeman, and Y.S. Wu, Phys. Rev. A **58**, 521 (1998).
[5] M.J. DeWitt, E. Wells, and R.R. Jones, Phys. Rev. Lett. **87**, 153001 (2001).
[6] E. Wells, M.J. DeWitt, and R.R. Jones, Phys. Rev. A **66**, 013409 (2002).
[7] H.R. Reiss, Phys. Rev. A **22**, 1786 (1980).
[8] J. Muth-Bohm, A. Becker, and F.H.M. Faisal, Phys. Rev. Lett. **85**, 2280 (2000).
[9] X. Chu and S.I. Chu, Phys. Rev. A **63**, 013414 (2001).
[10] A. Saenz, J. Phys. B **33**, 4365 (2000).
[11] M. Plummer and J.F. MaCann, J. Phys. B **30**, L401 (1997).
[12] C. Guo, Phys. Rev. Lett. **85**, 2276 (2000).
[13] F. Grasbon, G.G. Paulus, S.L. Chin, H. Walther, J. Muth-Bhm, A. Becker, and F.H.M. Faisal, Phys. Rev. A **65**, 041402(R) (2001).
[14] M. Lewenstein, P. Balcou, M.Y. Ivanov, A.L. Huillier, and P.B. Corkum, Phys. Rev. A **49**, 2117 (1994).
[15] B. Shan, A. Cavalieri, and Z. Chang (unpublished).
[16] B.M. Smirnov and M.I. Chibisov, Zh. Eksp. Teor. Fiz. **49**, 841 (1965) [Sov. Phys. JETP **22**, 585 (1966)].
[17] A.M. Perelomov, V.S. Popov, and M.V. Terentev, Zh. Eksp. Teor. Fiz. **50**, 1393 (1966) [Sov. Phys. JETP **23**, 924 (1966)].
[18] X.M. Tong and S.I. Chu, Int. J. Quantum Chem. **69**, 293 (1998).
[19] X.M. Tong and S.-I. Chu, Phys. Rev. A **64**, 013417 (2001).
[20] D. Dill and J.L. Dehmer, J. Chem. Phys. **61**, 192 (1974).
[21] X.L. Liang, X.C. Pan, and J.M. Li, Chin. Phys. Lett. **2**, 545 (1985).
[22] X.C. Pan, X.L. Liang, and J.M. Li, Acta Phys. Sin. **36**, 426 (1987).
[23] X.M. Tong and S.I. Chu, Phys. Rev. A **55**, 3406 (1997).
[24] X. Chu and S.-I. Chu, Phys. Rev. A **64**, 063404 (2001).
[25] A. Saenz, Phys. Rev. A **61**, 051402(R) (2000).
[26] S. Augst, D.D. Meyerhofer, D. Strickland, and S.L. Chin, J. Opt. Soc. Am. B **8**, 858 (1991).
[27] T.D.G. Walsh, F.A. Ilkov, J.E. Decker, and S.L. Chin, J. Phys. B **27**, 3767 (1994).
[28] J. Kobus, L. Laaksonen, and D. Sundholm, Comput. Phys. Commun. **98**, 346 (1996).
[29] G. Herzberg, *Molecular Spectra and Molecular Structure*, 2nd ed, Spectra of Diatomic Molecular Vol. 1 (Litton educational, New York, 1950).
[30] C. Guo, M. Li, J.P. Nibarger, and G.N. Gibson, Phys. Rev. A **58**, R4271 (1998).
[31] Y. Liang, A. Talebpour, C.Y. Chien, S. Augst, and S.L. Chin, J. Phys. B **30**, 1369 (1997).